black-and-white bars at the neuron's preferred orientation. The central region of the stereogram completely covered the minimum response field. After testing with RDS, neurons were classified as simple or complex on the basis of the modulation in their firing to drifting gratings[17]. Of the 72 neurons, 57 were tested in this way, of which 50 were complex cells and 7 were simple cells.

Analysis. For each neuron, the mean firing rate as a function of disparity ($f(d)$) was fitted with a Gabor function:

$$f(d) = A\exp(-(d-D)^2/2\sigma^2)\cos(2\pi\omega(d-D)+\phi)+B$$

by nonlinear regression, where A, ω and ϕ are the amplitude, spatial frequency and phase, respectively, of the cosine component, σ is the standard deviation of the gaussian, D is a position offset, and B is the baseline firing rate. In our model, this baseline firing corresponds to the activity produced by uncorrelated random-dot patterns. The correlated and anticorrelated data were fitted simultaneously, using the same values of B, ω, σ and D, but different values of A and ϕ (A_c, A_a, ϕ_c, ϕ_a, where the subscripts c and a refer to correlated and anticorrelated fits, respectively). The way in which changing from correlated to anticorrelated stimuli altered the disparity tuning of a single neurons could therefore be summarized by two parameters: an amplitude ratio A_a/A_c and a phase difference $\phi_c - \phi_a$. For the model complex cell, the amplitude ratio was 1.0 and the phase difference was π.

Received 10 February; accepted 23 June 1997.

1. Crick, F. & Koch, C. Are we aware of neural activity in primary visual cortex? *Nature* **375,** 121–123 (1995).
2. Julesz, B. *Foundations of Cyclopean Perception* (University of Chicago Press, 1971).
3. Cogan, A. I., Lomakin, A. J. & Rossi, A. Depth in anticorrelated stereograms. *Vision Res.* **33,** 1959–1975 (1993).
4. Masson, G. S., Busettini, C. & Miles, F. A. Vergence eye movements in response to binocular disparity without depth perception. *Nature* **389,** 283–286 (1997).
5. Marr, D. & Poggio, T. A computatonal theory of human stereo vision. *Proc. R. Soc. Lond. B* **204,** 301–328 (1979).
6. Grimson, W. E. L. A computer implementation of a theory of human stereo vision. *Phil. Trans. R. Soc. Lond. B* **292,** 217–253 (1981).
7. Barlow, H. B., Blakemore, C. & Pettigrew, J. D. The neural mechanisms of binocular depth discrimination. *J. Physiol. (Lond.)* **193,** 327–342 (1967).
8. Nikara, T., Bishop, P. O. & Pettigrew, J. D. Analysis of retinal correspondence by studying receptive fields of binocular single units in cat striate cortex. *Exp. Brain Res.* **6,** 353–372 (1968).
9. Poggio, G., Motter, B. C., Squatrito, S. & Trotter, Y. Responses of neurons in visual cortex (V1 and V2) of the alert macaque to dynamic random dot stereograms. *Vision Res.* **25,** 397–405 (1985).
10. Ohzawa, I., DeAngelis, G. C. & Freeman, R. D. Stereoscopic depth discrimination in the visual cortex: Neurons ideally suited as disparity detectors. *Science* **249,** 1037–1041 (1990).
11. Qian, N. Computing stereo disparity and motion with known binocular properties. *Neural Computat.* **6,** 390–404 (1994).
12. Poggio, G. F., Gonzalez, F. & Krause, F. Stereoscopic mechanisms in monkey visual cortex: binocular correlation and disparity selectivity. *J. Neurosci.* **8,** 4531–4550 (1988).
13. Poggio, G. & Poggio, T. The analysis of stereopsis. *Annu. Rev. Neurosci.* **7,** 379–412 (1984).
14. Poggio, G. F. & Fisher, B. Binocular interactions and depth sensitivity in striate and prestriate cortex of behaving rhesus monkey. *J. Neurophysiol.* **40,** 1392–1405 (1977).
15. Poggio, G. Mechanisms of stereopsis in monkey visual cortex. *Cerebr. Cort.* **3,** 193–204 (1995).
16. Judge, S. J., Richmond, B. J. & Chu, F. C. Implantation of magnetic search coils for measurement of eye position: an improved method. *Vision Res.* **30,** 535–538 (1980).
17. Skottun, B. C. *et al.* Classifying simple and complex cells on the basis of response modulation. *Vision Res.* **31,** 1079–1086 (1991).

Acknowledgements. This work was supported by the Wellcome Trust and the Royal Society.

Correspondence and requests for materials should be addressed to B.G.C. (e-mail: bc@physiol.ox.ac.uk).

Vergence eye movements in response to binocular disparity without depth perception

G. S. Masson*, C. Busettini & F. A. Miles

Laboratory of Sensorimotor Research, National Eye Institute, National Institutes of Health, Bethesda, Maryland 20892, USA
** Centre de Recherche en Neurosciences Cognitives, Centre National de la Recherche Scientifique, 13402 Marseille, France*

Primates use vergence eye movements to align their two eyes on the same object and can correct misalignments by sensing the difference in the positions of the two retinal images of the object (binocular disparity). When large random-dot patterns are viewed dichoptically and small binocular misalignments are suddenly imposed (disparity steps), corrective vergence eye movements are elicited at ultrashort latencies[1,2]. Here we show that the same steps applied to dense anticorrelated patterns, in which each black dot in one eye is matched to a white dot in the other eye, initiate vergence responses that are very similar, except that they are in the opposite direction. This sensitivity to the disparity of anticorrelated patterns is shared by many disparity-selective neurons in cortical area V1 (ref. 3), despite the fact that human subjects fail to perceive depth in such stimuli[4,5]. These data indicate that the vergence eye movements initiated at ultrashort latencies result solely from locally matched binocular features, and derive their visual input from an early stage of cortical processing before the level at which depth percepts are elaborated.

Disparity-selective neurons have often been implicated in the perception of depth (stereopsis)[6], and it has been shown that in the first stage of the cortical visual pathways in area V1, such neurons are sensitive to the disparity of anticorrelated patterns[3], even though such patterns are perceptually rivalrous, cannot be fused, and lack consistent depth[4,5]. Furthermore, the disparity tuning curves of the neurons were often inverted with anticorrelated patterns, a characteristic of simple local filtering models[7,8]. These findings are consistent with the hypothesis that these neurons respond to purely local matches between the images seen by the two eyes, regardless of whether a global match is present[9]. Thus, such neurons do not solve the correspondence problem and can represent only a rudimentary stage in the processing of binocular signals for stereopsis. We now provide evidence that such rudimentary binocular signals can generate motor responses by showing that small disparity stimuli applied to dense anticorrelated patterns give rise to inverted vergence eye movements at ultrashort latencies.

A variety of cues can be used to control the angle of convergence between the two lines of sight[10,11], but the only cue of concern here is binocular disparity[1,12], which provides a direct measure of the misalignment of the two eyes with respect to the object(s) of interest (vergence error) and is assumed to be sensed directly by disparity-selective neurons[13,14]. Examples of the initial vergence responses elicited by small horizontal disparities ($<2°$) applied to large correlated random-dot patterns (matching images at the two eyes) are seen in Fig. 1 (continuous line), which shows mean vergence velocity profiles for one human (Fig. 1a) and for one monkey (Fig. 1c). Stimuli were presented on a tangent screen using two slide projectors and orthogonal polarizing filters to allow independent control of the images seen by each eye. Each trial started with the screen blank and then stationary patterns with a given horizontal disparity were presented. For the data shown in Fig. 1a, c, all patterns had crossed disparities (the pattern seen by the right eye had been shifted leftwards; the pattern seen by the left eye had been shifted rightwards), simulating the abrupt appearance of a textured surface in front of the tangent screen. Such stimuli initiated increased convergence—the correct response to restore binocular alignment—with a latency of <60 ms in the case of the monkey and <90 ms in the case of the human[1,2]. The initial vergence responses to anticorrelated random-dot patterns with similar crossed disparities are shown as dotted lines in Fig. 1a, c and are clearly in the reverse direction. These inverted responses have a comparably short latency but a slightly lower rate of acceleration.

We quantified these initial motor responses by measuring the change in vergence position over a 33-ms period commencing at a fixed time after the appearance of the disparity stimuli: 60 ms for the monkey, 90 ms for the human. This meant that our measures were restricted to the initial (open-loop) vergence responses that were generated by the disparity input before it had been affected by eye-movement feedback. Disparity tuning curves based on these measures are plotted in Fig. 1b (human) and Fig. 1d (monkey), and show the characteristic S-shapes with non-zero asymptotes[1], consistent with the operation of a depth-tracking servo of modest range. Thus, with normal (correlated) patterns and disparities up to a degree or two, the slopes are positive and small increases in the

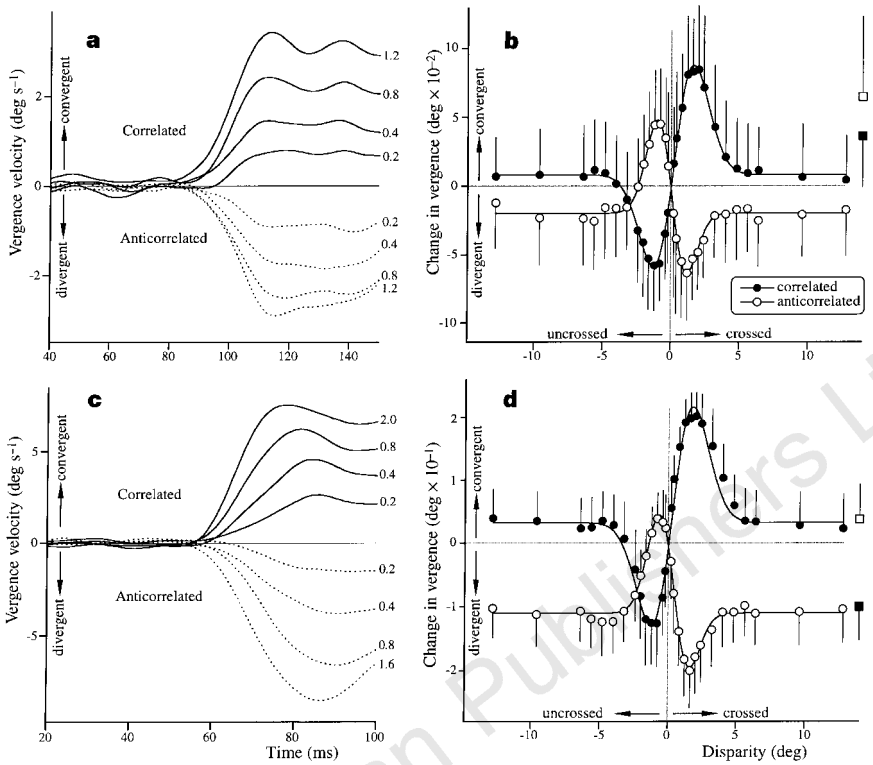

Figure 1 Vergence eye movements elicited by disparity stimuli applied to high-density random-dot patterns (50%). **a**, Mean vergence velocity responses of human subject, F.A.M., to crossed disparity stimuli applied to correlated (continuous line) and anticorrelated (dotted line) patterns, with stimulus magnitudes (in degrees) at the ends of traces. Note, vergence velocity is the difference between velocity of the two eyes (left eye–right eye) and increasing convergence is positive (upward deflection). **b**, Plot of mean (±s.d.) changes in vergence position (over period 90–123 ms, starting from stimulus onset) against disparity stimulus for human subject, F.A.M., with correlated (filled circles) and anticorrelated (open circles) patterns; also shown are control responses to zero-disparity stimuli applied to correlated (filled square) and anticorrelated (open square) patterns. **c**, Mean vergence velocity responses of monkey, Bo, in response to crossed disparity stimuli. **d**, Plot of mean (±s.d.) changes in vergence (over period 60–93 ms from stimulus onset) for monkey, Bo. Individual traces and datum points based on at least 178 responses.

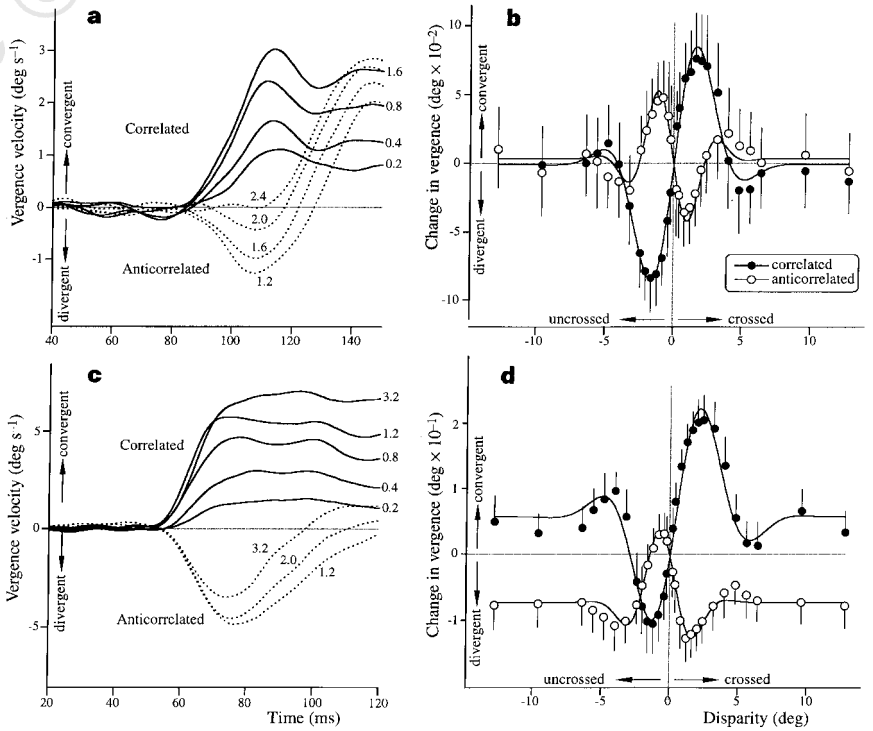

Figure 2 Vergence eye movements elicited by disparity stimuli applied to low-density random-dot patterns (7.5%). Layout, subjects and conventions all identical to Fig. 1. Individual traces and datum points based on at least 84 responses.

Table 1 Best-fit Gabor parameters

Subject	A	σ	D	ω	ϕ	B	R
Correlated patterns							
F.A.M.	0.39	1.48	0.27	0.0337	271.6	0.008	0.146
R.J.K.	0.35	1.69	0.20	0.0353	272.3	0.002	0.156
Bo	0.93	1.53	0.32	0.0324	271.2	0.032	0.346
Lu	0.94	1.58	0.12	0.0189	270.4	–0.002	0.212
Ch	0.49	1.84	1.33	0.0667	278.8	0.150	0.420
Anticorrelated patterns							
F.A.M.	0.58	1.08	–0.02	0.0234	88.0	–0.020	0.112
R.J.K.	0.45	1.13	0.30	0.0198	89.1	–0.024	0.077
Bo	0.83	1.12	0.29	0.0336	85.9	–0.111	0.241
Lu	0.53	1.09	–0.25	0.0270	85.3	–0.014	0.123
Ch	1.23	1.03	0.95	0.0250	86.3	–0.153	0.249

Best-fit parameters when the following Gabor function was fitted to the disparity tuning curves obtained with high-density random-dot patterns (50%):

$$f(d) = A \exp\left(-\frac{(d-D)^2}{2\sigma^2}\right)\cos\left(2\pi\omega(d-D)+\phi\right)+B$$

where d is the stimulus disparity, A is a gain factor, σ is the gaussian width, ω and ϕ are the spatial frequency and phase of the cosine term, D is the displacement, and B is an offset parameter to allow for the non-zero asymptotes. An iterative procedure with a least-squares criterion was used to obtain the best fits with each of the parameters resolved to the number of decimal places shown. R is the peak-to-peak amplitude derived from the best-fit Gabor functions. All units are in degrees except for ω, which is in cycles per deg. Data are for two human subjects (F.A.M., R.J.K.) and three monkeys (Bo, Lu, Ch).

magnitude of the stimulus (disparity) lead to roughly proportional increases in the magnitude of the response (vergence) in the appropriate direction: crossed disparities elicit increased convergence and uncrossed disparities decreased convergence. Larger disparities exceed the system's operating range and responses default towards a non-zero level that is idiosyncratic and might reflect residual correlations[1]. In contrast, the disparity tuning curves obtained with anticorrelated patterns are almost mirror images of those obtained with correlated patterns. Similar clear evidence for a sign inversion with anticorrelated patterns was obtained for two more monkeys and one more human.

The curves in Fig. 1b,d are least-squares-fit Gabor functions, with an offset term to allow for the non-zero asymptotes. Such functions are commonly used in vision research to characterize linear filters and they provide a good fit to our data, allowing an objective quantitative comparison of the responses to correlated and anticorrelated patterns. The parameters for these fits, together with those for the additional subjects, are listed in Table 1. To give some estimate of the amplitude of modulation with disparity, Table 1 includes the peak-to-peak amplitude of the Gabor functions (R). (This derived measure was used because it describes the amplitude of modulation reliably, independent of any one term in the fitted function. Note that the spatial frequencies, ω, are always very low so that, within the important disparity range, $\pm 5°$, the cosine terms are almost linear and pass very close to the origin, with positive slopes for the correlated data and negative slopes for the anticorrelated data.) The amplitude measure (R) and the gaussian width (σ) were invariably smaller with the anticorrelated patterns than they were with the correlated patterns, on average by 37% (range, 23–51%) and 32% (range, 27–44%), respectively. The sign inversion is evident from the difference in the phase of the cosine terms (ϕcorrelated − ϕanticorrelated), which generally approximated π: 183.6° (human subject F.A.M.), 183.2° (human R.J.K.), 185.3° (monkey Bo), 185.1° (monkey Lu) and 192.5° (monkey Ch). The data for the two species were similar in all essentials, indicating that the monkey is a good animal model for the human.

The preceding paper[3] shows that many neurons in V1 respond to the local matches in anticorrelated patterns, often with a sign inversion, and we have shown here that these patterns can elicit vergence eye movements with a sign inversion at ultrashort latencies. We think it likely that the two observations are causally linked: that is, the earliest vergence eye movements derive their visual input from an early stage of cortical processing, possibly even as early as V1 (ref. 15). Cortical disparity-selective neurons that might drive vergence have been classified as 'near', 'far', 'tuned-near' and 'tuned-far', depending on the range of disparities over which they are active[14]. The vergence response to a given disparity in our experiments is determined by the net balance of activity in the population of these disparity-selective neurons that influences the vergence state. The preceding paper[3] helps to explain how this balance is likely to differ with correlated and anticorrelated patterns. For example, consider the neurons like those in Fig. 3 of ref. 3, whose disparity tuning curves are inverted with anticorrelated patterns (and whose Gabor fits show a phase difference of roughly π). The subset of such neurons that is maximally active when a given disparity is applied to the correlated patterns, for example, will be minimally active when that same disparity is applied to the anticorrelated patterns (and vice versa). In fact, the balance of activity within the whole population of such neurons when a given disparity is applied to an anticorrelated pattern will be the mirror image of that obtained when the same disparity is applied to a correlated pattern. The net result is to change the sign of the disparity feedback signal driving vergence: if the balance of activity when a given disparity is applied to the correlated pattern results in increased convergence, then the balance when that same disparity is applied to the anticorrelated pattern would result in decreased convergence and vice versa. Such neurons might therefore explain our inverted vergence data with anticorrelated patterns, although we cannot rule out a contribution from neurons that show phase shifts of less than π with anticorrelated stimuli. Note that, because we are dealing with a population response, the Gabor parameters for vergence eye movements need not be expected to match the Gabor parameters for any given cell type.

From the functional standpoint, the sensitivity to anticorrelated patterns indicates that the sensory mechanisms underlying the vergence eye movements studied here deal solely with local disparity matches, regardless of the global disparity match, and consequently do not solve the correspondence problem. This is in line with our previous suggestion that these reflex-like vergence mechanisms normally function only to eliminate small (residual?) vergence errors, merely passively aligning the two eyes on the nearest available salient object(s)[1]. Additional mechanisms are needed to transfer gaze actively to new depth planes, which in a crowded visual world requires target selections that must often pose a correspondence problem. This seems likely to involve higher-level processing and to require much more time, perhaps accounting for the much longer latencies—160 ms or more—generally reported for vergence eye movements[12,16,17]. Evidence for an intermediate stage of processing comes from some additional experiments that we have done with low-density random-dot patterns. All of the data described so far were obtained with random dots that covered 50% of the image space, but we also tested four subjects with patterns in which the dots were more sparsely distributed. Reducing the dot density to 7.5% (by reducing the number of dots) had little effect on the vergence eye movements elicited with correlated patterns, but the inverted responses recorded with anticorrelated patterns were now very transient (see Fig. 2: same layout as for Fig. 1). In fact, with these anticorrelated patterns, the vergence velocity profiles were now biphasic, the initial reversal lasting only 30–60 ms and being replaced by a 'correctly' directed response. The latter ranged from robust (as in Fig. 2a) to very weak (as in Fig. 2c), and presumably resulted from a later, more global stage of processing by neurons that respond to spatial matching independently of contrast. When dot density was further reduced to 0.6% (by also reducing dot size) these later 'correctly' directed responses became a consistent feature, whereas the initial transient reversals were seen in only 3 of the 8 data sets (not shown). This is in accord with our well known ability to initiate appropriately directed vergence eye movements to small single-line stimuli that have opposite contrast at the two eyes[16,18].

In a two-alternative forced-choice procedure, three human observers (two of whom were naive) were able correctly to discriminate 1.2° crossed and uncrossed disparities applied to our correlated patterns, regardless of dot density. None of the subjects was able to make these discriminations with our denser anticorrelated patterns (50 and 7.5%), even when a central (binocular) fixation spot remained available on the screen as a reference to allow a relative depth judgement[19]. However, all of the subjects were able to make these discriminations (correctly) with the least-dense anticorrelated patterns (0.6%), with or without the reference spot. These findings are all in agreement with a previous study[5] which showed that some subjects can perceive depth in low-density anticorrelated patterns (<5%). Our data with dense patterns provide a clear instance of a dissociation between sensory perception (depth) and motor responses (short-latency vergence). This is consistent with the idea that the earliest vergence responses reported here depend on inputs derived from an early stage of cortical processing. □

Methods

Vergence eye movements. Most techniques have been described previously[1,20]. The positions of both eyes were recorded using the electromagnetic search coil technique[21]. Subjects faced a tangent screen (viewing distance 33 cm; subtense, 80° × 80°) onto which two random-dot patterns were simultaneously back-projected. Patterns could be (1) high-density (2° diameter dots covering 50% of the image space) or (2) low-density (2° dots with 7.5% coverage, or 0.5° dots with 0.6% coverage), with the additional constraint that dot centres had minimal separations of 5°. Orthogonal polarizing filters in the projection paths ensured that each of the two eyes saw only one of the patterns, the horizontal positioning of which was controlled by mirror galvanometers. For high-density correlated stimuli, patterns seen by each eye had matching black dots on a white background. For high-density anticorrelated stimuli, the left eye saw black dots on a white background and the right eye saw a matching negative image (white dots on a black background). The low-density patterns were similarly arranged, except that the dots always appeared against a grey background. Trials started with the screen blank (same space-averaged luminance as for the patterns), except for a target spot projected onto the screen 10° right of centre, which the subject was required to fixate. After a randomized interval this spot was extinguished and a second appeared at the centre of the screen. Subjects were required to make a saccadic eye movement to acquire this new target, at which time the target was switched off. With gaze now directed at the screen centre, stationary random-dot patterns with a fixed disparity appeared (post-saccadic delay: 30 ms for monkeys and 50 ms for humans) for a brief period (100 ms for monkeys and 200 ms for humans) before the screen was blanked, ending the trial. This procedure served to apply the disparity stimuli in the wake of centring saccades to take advantage of post-saccadic enhancement[1,2]. Disparities ranged from 0 to 12.8° (crossed and uncrossed, correlated and anticorrelated patterns) and varied randomly from trial to trial. All data shown have had the responses to zero disparities (plotted separately as square symbols in Fig. 1b, c) subtracted to eliminate any post-saccadic vergence drifts and idiosyncratic responses to the mere appearance of a pattern. This has the effect of forcing all the disparity tuning curves through the origin.

Psychophysical tests of depth discrimination. In a two-alternative forced-choice procedure, human subjects were asked to indicate whether a random-dot pattern appeared nearer or farther from the projection screen when subjected to 1.2° crossed and uncrossed disparities for 200 ms, exactly as in the experiments described above. Because our patterns provide only absolute disparity cues, trials were also included in which a central fixation spot remained available as a reference[19].

Received 10 February; accepted 27 June 1997.

1. Busettini, C., Miles, F. A. & Krauzlis, R. J. Short-latency disparity vergence responses and their dependence on a prior saccadic eye movement. *J. Neurophysiol.* **75,** 1392–1410 (1996).
2. Busettini, C., Miles, F. A. & Krauzlis, R. J. Short-latency disparity vergence responses in humans. *Soc. Neurosci. Abstr.* **20,** 1403 (1994).
3. Cumming, B. G. & Parker, A. J. Responses of primary visual cortical neurons to binocular disparity without depth perception. *Nature* **389,** 280–283 (1997).
4. Julesz, B. Binocular depth perception of computer-generated patterns. *Bell System Tech. J.* **39,** 1125–1162 (1960).
5. Cogan, A. I., Lomakin, A. J. & Rossi, A. F. Depth in anticorrelated stereograms: Effects of spatial density and interocular delay. *Vision Res.* **33,** 1959–1975 (1993).
6. Bishop, P. O. & Pettigrew, J. D. Neural mechanisms of binocular vision. *Vision Res.* **26,** 1587–1600 (1986).
7. Ohzawa, I., DeAngelis, G. C. & Freeman, R. D. Stereoscopic depth discrimination in the visual cortex: neurons ideally suited as disparity detectors. *Science* **249,** 1037–1041 (1990).
8. Qian, N. Computing stereo disparity and motion with known binocular properties. *Neural Computat.* **6,** 390–404 (1994).
9. Parker, A. J. & Cumming, B. G. Local vs global stereoscopic matching in neurons of cortical area V1. *Invest. Ophthalmol. Vis. Sci.* **37,** S424 (1996).
10. Collewijn, H. & Erkelens, C. J. in *Eye Movements and their Role in Visual and Cognitive Processes* (ed. Kowler, E.) 213–261 (Elsevier, Amsterdam, 1990).
11. Judge, S. J. in *Vision and Visual Dysfunction, 8: Eye Movements* (ed. Carpenter, R. H. S.) 157–172 (Macmillan, London, 1991).
12. Rashbass, C. & Westheimer, G. Disjunctive eye movements. *J. Physiol. (Lond.)* **159,** 339–360 (1961).
13. Poggio, G. F. & Fischer, B. Binocular interaction and depth sensitivity in striate and prestriate cortex of behaving rhesus monkey. *J. Neurophysiol.* **40,** 1392–1405 (1977).
14. Poggio, G. F. Mechanisms of stereopsis in monkey visual cortex. *Cerebr. Cort.* **5,** 193–204 (1995).
15. Trotter, Y., Celebrini, S., Stricanne, B., Thorpe, S. & Imbert, M. Neural processing of stereopsis as a function of viewing distance in primate visual cortical area VI. *J. Neurophysiol.* **76,** 2872–2885 (1996).
16. Mitchell, D. E. Properties of stimuli eliciting vergence eye movements and stereopsis. *Vision Res.* **10,** 145–162 (1970).
17. Cumming, B. G. & Judge, S. J. Disparity-induced and blur-induced convergence eye movement and accommodation in the monkey. *J. Neurophysiol.* **55,** 896–914 (1986).
18. Westheimer, G. & Mitchell, D. E. The sensory stimulus for disjunctive eye movements. *Vision Res.* **9,** 749–755 (1969).
19. Regan, D., Erkelens, C. J. & Collewijn, H. Necessary conditions for the perception of motion in depth. *Invest. Opthalmol. Vis. Sci.* **27,** 584–597 (1986).
20. Busettini, C., Miles, F. A., Schwarz, U. & Carl, J. R. Human ocular responses to translation of the observer and of the scene: dependence on viewing distance. *Exp. Brain Res.* **100,** 484–494 (1994).
21. Fuchs, A. F. & Robinson, D. A. A method for measuring horizontal and vertical eye movement chronically in the monkey. *J. Appl. Physiol.* **21,** 1068–1070 (1966).

Acknowledgements. G.S.M. was supported by La Fondation pour la Recherche Medicale (France).

Correspondence and requests for materials should be addressed to F.A.M. (e-mail: fam@lsr.nei.nih.gov).

Action-potential propagation gated by an axonal I_A-like K^+ conductance in hippocampus

Dominique Debanne*, Nathalie C. Guérineau*, Beat H. Gähwiler & Scott M. Thompson

Brain Research Institute, August Forel-Strasse 1, CH-8029 Zurich, Switzerland

Integration of membrane-potential changes is traditionally reserved for neuronal somatodendritic compartments. Axons are typically considered to transmit reliably the result of this integration, the action potential[1], to nerve terminals[2,3]. By recording from pairs of pyramidal cells in hippocampal slice cultures[4–6], we show here that the propagation of action potentials to nerve terminals is impaired if presynaptic action potentials are preceded by brief or tonic hyperpolarization. Action-potential propagation fails only when the presynaptic action potential is triggered within the first 15–20 ms of a depolarizing step from hyperpolarized potentials; action-potential propagation failures are blocked when presynaptic cells are impaled with electrodes containing 4-aminopyridine, indicating that a fast-inactivating, A-type K^+ conductance is involved. Propagation failed between some, but not all, of the postsynaptic cells contacted by a single presynaptic cell, suggesting that the presynaptic action potentials failed at axonal branch points. We conclude that the physiological activation of an I_A-like potassium conductance can locally block propagation of presynaptic action potentials in axons of the central nervous system. Thus axons do not always behave as simple electrical cables: their capacity to transmit action potentials is determined by a time-dependent integration of recent membrane-potential changes.

* Present addresses: Unité de Neurocybernétique Cellulaire, UPR9041 CNRS, 280 Bld Sainte Marguerite, 13009 Marseille, Franc (D.D.) CCIPE, U469 INSERM, 141 rue de la Cardonille, 34094 Montpellier CEDEX 5, France (N.C.G.).